Near-complete transmission through subwavelength hole arrays in phonon-polaritonic thin films

Peter B. Catrysse and Shanhui Fan
Department of Electrical Engineering, Stanford University, Stanford, California 94305-4088, USA
(Received 9 November 2006; revised manuscript received 16 January 2007; published 26 February 2007)

We report that phonon-polaritonic thin films with a periodic array of subwavelength holes allow near-complete transmission in the polariton gap where a homogeneous film completely suppresses transmission. We find that both propagating modes inside the subwavelength holes and surface resonances on the film interfaces play a crucial role in the transmission behavior. In the frequency range where both occur simultaneously, they interfere destructively and completely suppress transmission. When both mechanisms are spectrally separated, each individually results in enhanced transmission.

DOI: 10.1103/PhysRevB.75.075422 PACS number(s): 78.20.Ci, 42.79.Dj, 71.36.+c

Enhanced transmission through subwavelength holes in an otherwise opaque medium has captured great interest due to its fundamental importance for manipulating light at small length scales, as well as its practical significance for photonic devices and applications including near-field microscopy, optical filtering, lithography, and high-density optical data storage.[1–3]

In the visible wavelength range, where the plasmonic response of metals is prominent, the effect of enhanced transmission is intricately connected to the presence of surface plasmon polaritons.[1,4–7] At lower frequencies, the plasmonic response of metals is either far weaker or nonexistent. Therefore, in the longer-wavelength range ($>100\ \mu$m), one instead relies on doped semiconductors that exhibit plasmonic response in the terahertz regime[8] or structured perfect electrical conductor surfaces that spoof surface plasmons for microwaves.[9] However, at midinfrared wavelengths ($\sim 10\ \mu$m), there is no strong plasmonic response from either metals or semiconductors. Yet, enhancing transmission in this wavelength range is still very important. For example, many molecules have unique spectral signatures in the midinfrared. Field concentration, associated with enhanced transmission through subwavelength holes in an otherwise opaque medium, can be very beneficial for infrared spectroscopic studies where highly localized fields are required in the vicinity of the film.[10,11]

Here, we propose to use the phonon-polaritonic response to enhance optical transmission through subwavelength hole arrays in an otherwise opaque thin film. A periodic array of subwavelength holes is shown to allow near-complete transmission inside the polariton gap, where a homogeneous film made out of a phonon-polaritonic medium completely suppresses transmission. Moreover, the phonon-polariton modes in this system have very different dispersion behaviors compared with plasmon polaritons in metallic systems. The differences in dispersion result in very distinct features in the transmission spectrum. For example, the Rayleigh-Wood anomaly, which is typically present in metallic systems, disappears from the regime of enhanced transmission in a phonon-polaritonic system. More surprisingly, in contrast with metallic systems, it turns out that surface phonon polaritons on interfaces and propagating modes in subwavelength holes always coincide in the same spectral regime, leading to pronounced interference effects.

In phonon-polaritonic media, a transverse optical phonon and a transverse electromagnetic wave can couple to create a polariton gap, in which the propagation of electromagnetic waves is prohibited. This behavior is represented by a frequency-dependent dielectric function,[12]

$$\varepsilon_1(\omega) = \varepsilon_\infty \frac{\omega_L^2 - \omega^2 + i\gamma\omega}{\omega_T^2 - \omega^2 + i\gamma\omega}, \tag{1}$$

where ω represents the (angular) frequency, ε_∞ is the high-frequency dielectric response, ω_T is the transverse optical phonon frequency, ω_L is related to ε_∞ and ω_T through the Lyddane-Sachs-Teller relation,[12] and γ is a measure of material losses. Equation (1) proves to be extremely accurate for bulk silicon carbide (SiC) at infrared wavelengths between 2 and 22 μm with $\varepsilon_\infty = 6.7$, $\omega_T = 2\pi c \times (793\ \mathrm{cm}^{-1})$, $\omega_L = 2\pi c \times (969\ \mathrm{cm}^{-1})$, and $\gamma = 2\pi c \times (4.76\ \mathrm{cm}^{-1})$, where c denotes the speed of light in vacuum.[13]

Inside the polariton gap, the real part of $\varepsilon_1(\omega)$ is negative and a SiC-dielectric interface supports surface waves, i.e., surface phonon polaritons (SPPs) with wave vectors $k_{\mathrm{SPP}}(\omega)$ related to the wave frequency ω by the following dispersion relation;

$$k_{\mathrm{SPP}}(\omega) = \frac{\omega}{c}\sqrt{\frac{\varepsilon_1(\omega)\varepsilon_2}{\varepsilon_1(\omega) + \varepsilon_2}}, \tag{2}$$

as shown in Fig. 1(a) for a SiC-air interface ($\varepsilon_2 = 1$). We note that SPPs cover most of the bandwidth inside the polariton gap from $\omega_T = 0.82\omega_L$ to ω_L with a group velocity rapidly varying from $c/\sqrt{\varepsilon_2}$ to 0. As we will show explicitly later, the SPP region [red curve in Fig. 1(a)] also corresponds to the regime of enhanced transmission. In contrast, Fig. 1(b) shows the dispersion relation for surface plasmon polaritons on a metal-air interface (blue curve; ω_p is the plasma frequency of the metal). While it covers the entire frequency range from 0 to $\omega_p/\sqrt{2}$, enhanced transmission studies in metallic systems typically occur in the frequency range where surface plasmons exhibit low losses, i.e., where the plasmon-polariton dispersion relation does not substantially deviate from the light line in air [red curve in Fig. 1(b)]. This is especially true when applying metals in the midinfrared, see for example Ref. 11. As a consequence, the excited surface waves are highly delocalized and extend far away from the metal film. In contrast, the surface phonon polariton is strongly confined to the interface at midinfrared wavelengths and the strong field localization is preserved. It is these dispersion differences for surface waves on phonon-polaritonic

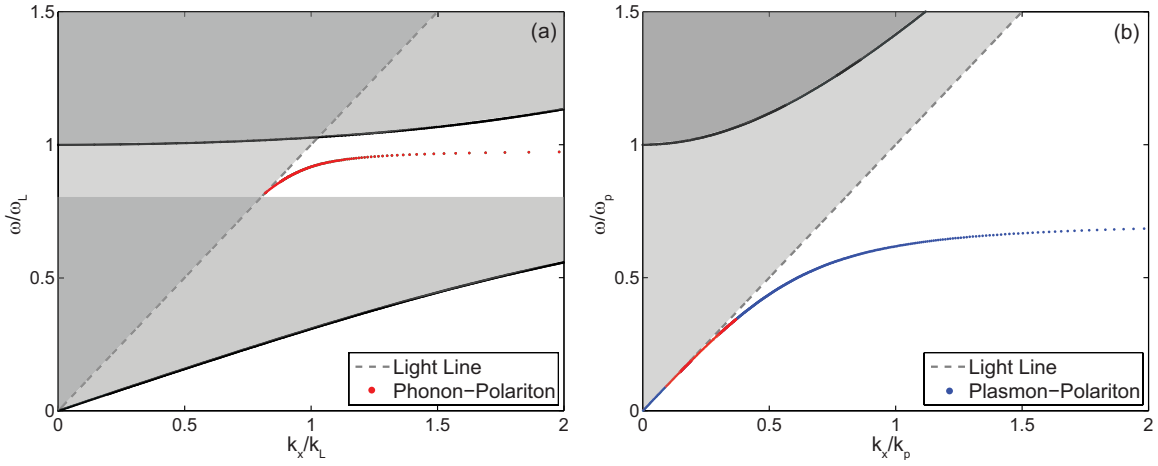

FIG. 1. (Color) Dispersion relations for (a) surface phonon-polaritons ($k_L=\omega_L/c$) and (b) surface plasmon-polaritons ($k_p=\omega_p/c$) on a single interface with air. Red curves indicate regimes of enhanced transmission. Black curves depict the bulk dispersive properties [$k(\omega)=\sqrt{\varepsilon(\omega)}\omega/c$]. Shaded areas represent the continuum of modes extended in the respective materials: (a) in air and in the bulk phonon-polaritonic material outside the polariton gap and (b) in air and in the bulk plasmonic material above the plasma frequency. Dashed gray lines represent the light line in air.

and plasmon-polaritonic materials that directly influence their behavior and role in the regime of enhanced transmission.

Using a three-dimensional (3D) finite-difference time-domain (FDTD) method,[14] we numerically investigate the transmission through SiC thin films with a periodic array of subwavelength holes for a normally incident plane wave. As a reference, we first calculate the transmission through a homogeneous SiC thin film of thickness $h=4$ μm (Fig. 2, dashed gray curve). Inside the polariton gap, between 10.32 and 12.59 μm, transmission is completely suppressed as expected. In contrast, the solid green curve depicts the transmission with a square lattice of subwavelength air holes in the film (Fig. 2 inset with period $a=10.4$ μm and radius $r_0=2.8$ μm). The spectrum features near-complete transmission from 11.5 to 12.5 μm and completely suppressed transmission between 11.08 and 11.33 μm. Both features are located entirely within the polariton gap of SiC.

From previous studies of metallic systems, it is known that surface resonances[1,5] and propagating modes inside the holes (sometimes referred to as localized or shape resonances)[15,16] can each provide separate pathways for

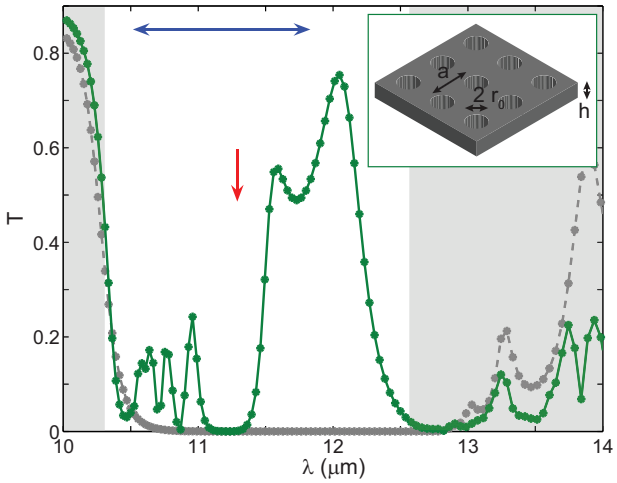

FIG. 2. (Color) Transmission at normal incidence through a SiC film with a two-dimensional periodic arrangement of subwavelength cylindrical holes (solid green curve). The inset shows the geometry with radius $r_0=2.8$ μm, period $a=10.4$ μm, and thickness $h=4$ μm. The dashed gray curve is the transmission spectrum of a homogeneous SiC film. The polariton gap is represented by clear region between the gray regions. The surface resonance is indicated by the red vertical arrow. The blue horizontal arrow shows the range of the propagating mode in the hole.

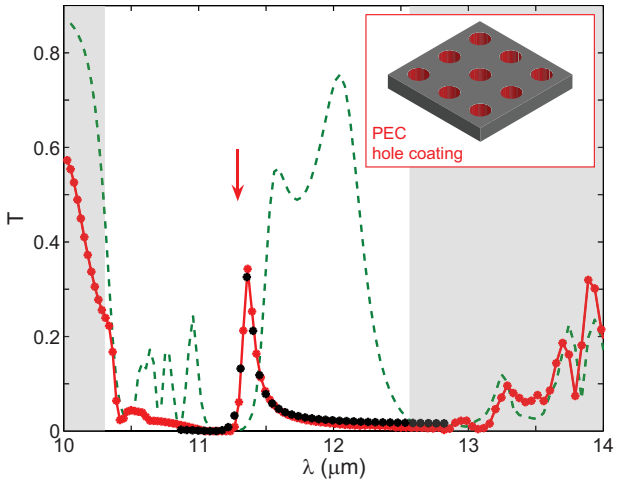

FIG. 3. (Color) Transmission at normal incidence through a SiC film with a two-dimensional periodic arrangement of subwavelength cylindrical holes with a perfect electric conductor (PEC) coating (solid red line). The inset shows the geometry with the 200 nm PEC coating in the holes indicated in red. The red vertical arrow indicates the surface resonance. Black dots represent the quantitative model for the transmission peak at 11.36 μm. The transmission spectrum in Fig. 1 is shown for reference (dashed green curve).

transmission through subwavelength hole arrays. In phonon-polaritonic systems, however, both pathways are always present simultaneously and their interplay must be studied in order to understand the complex transmission behavior.

Surface resonance. The use of surface resonances to enhance transmission in subwavelength hole arrays is well documented for metallic systems.[1,5] What is their role in transmission through phonon-polariton systems? In general, $k_{SPP}(\omega) > \sqrt{\varepsilon_2}\omega/c$ and SPPs are confined to the SiC-air interface; they cannot couple to far-field incident light. The presence of a periodic array, however, provides a phase-matching mechanism that allows surface waves to couple to normally incident light. For the array in Fig. 2, the frequencies ω_{mn} at which surface modes can be resonantly excited by a square lattice with period a are estimated using

$$|k_{SPP}(\omega_{mn})| = \sqrt{m^2 + n^2}\frac{2\pi}{a}, \tag{3}$$

where m and n are integers.[1] The lowest-order surface resonance (with $m=1$ and $n=0$ or $m=0$ and $n=1$) is excited at 11.29 μm (vertical red arrow in Figs. 2 and 3). In contrast to what has been observed in many metallic hole arrays, the surface resonance coincides with the range of 11.08–11.33 μm in which transmission is *completely suppressed* (Fig. 2). Moreover, due to the unique nature of the surface phonon-polariton dispersion relations, we find that $k_{SPP}(\omega) \gg \sqrt{\varepsilon_2}\omega/c$ in this region. Hence, Rayleigh-Wood anomalies,[17,18] associated with the appearing or disappearing of new diffraction orders at $\sqrt{\varepsilon_2}\omega/c = \sqrt{m^2+n^2}2\pi/a$, are entirely absent in the regime of enhanced transmission. In contrast, for surface plasmon polaritons in metallic systems $k_{SPP}(\omega) \approx \sqrt{\varepsilon_2}\omega/c$ and Rayleigh-Wood anomalies always spectrally coincide with surface resonances. Their presence leads to very strong variations in the transmission behavior, including suppression in the vicinity of transmission peaks for both slit and hole geometries.[6,7]

Propagating mode in the hole. In general, when an aperture supports propagating modes, these modes can form an efficient pathway for transmission.[4,15,16,19] To calculate the propagating modes inside a cylindrical hole, we treat the hole as a z-invariant waveguide with a circular cross section of radius r_0 in the transverse xy plane [Fig. 4(a), inset] and solve for the dispersion relation (λ, β), which describes the propagation constant along the hole β as a function of wavelength λ.[16] Such analysis reveals that a subwavelength hole in a phonon-polaritonic system always supports a propagating mode, regardless of how small the holes are. When $r_0 \to 0$, the cutoff frequency ω_c of the propagating modes asymptotically approaches the surface phonon frequency ω_{SP} inside the hole (determined by $-\mathrm{Re}[\varepsilon_1(\omega_{SP})] = \varepsilon_2$). Figure 4(a) shows the dispersion relation for the lowest-order propagating mode in an air-hole ($\varepsilon_2=1$) with radius $r_0=2.8$ μm surrounded by SiC (ε_1). Higher-order modes are present but do not couple effectively with normally incident light and are not plotted. The mode covers a wavelength range from 10.53 (ω_{SP}) to 11.42 μm (ω_c) and spectrally overlaps with both the near-complete transmission window and range of completely suppressed transmission.

Spectral analysis above has shown that both surface modes and propagating modes occur simultaneously in the spectral range of interest. Moreover, due to the unique dispersion properties of phonon-polaritonic media, the contributions from these distinct types of modes cannot be easily separated. To illustrate the role of each mechanism separately, we design computational experiments in which we selectively remove either one of the pathways by coating part of the structure with a thin layer of perfect electric conductor (PEC).

Enhanced transmission due to surface resonance only. To isolate the contribution of the surface resonance, we coat the curved vertical walls of the subwavelength holes with a 200 nm PEC layer while maintaining the hole radius at 2.8 μm (red area in the inset of Fig. 3). In a cylindrical PEC-air waveguide, the cutoff wavelength for the dominant TE_{11} mode is $3.41r_0=9.55$ μm.[20] Hence, the PEC coating completely eliminates the presence of propagating modes inside the polariton gap of SiC. The calculated transmission spectrum (Fig. 3, solid red curve) for this structure features a transmission peak at 11.36 μm, which is in good agreement with the location of the surface resonance predicted using Eq. (3), as well as a direct calculation of the location of the surface resonance using FDTD simulations that solve Maxwell's equations exactly in a numerical fashion without uncontrolled approximations (not shown). Therefore, in the absence of propagating modes inside the holes, the surface resonance alone serves as a pathway for transmission, which is consistent with previous studies in metallic systems.

Enhanced transmission due to propagating modes inside the holes only. To isolate the contribution of the propagating modes, we apply a 200 nm thin PEC coating to the top and bottom surfaces of the SiC film [blue area in the inset of Fig. 4(b)]. This prevents the excitation of SPP resonances on the flat SiC-air interfaces. (While a perforated PEC surface does support surface waves of its own, their resonance frequency, as determined by analytic theory in Ref. 9, lies outside of the polariton gap. This is also confirmed by our FDTD simulations.) As shown in Fig. 4(b), the structure exhibits a broad window of enhanced transmission with a Fabry-Pérot-type oscillation and coincides perfectly with the range predicted by the dispersion relation of a single hole [Fig. 4(a)]. Hence, in the absence of surface resonances, enhanced transmission is entirely due to a propagating mode inside the subwavelength holes.

Interplay between the two pathways. The mechanisms that lead to the transmission spectrum in Fig. 2 can now be illustrated in comparison with the results of the separate analyses of the surface resonance and the propagating mode shown in Figs. 3 and 4. The simultaneous presence of two transmission pathways leads to two very striking effects.

(a) Transmission is near-complete between 11.5 and 12.5 μm. This feature is due primarily to the excitation of propagating modes inside the holes. Even though the interaction between propagating modes and surface resonances leads to a strong shift of the high-transmission window to the longer-wavelength range, the oscillation due to Fabry-Pérot effects inside the hole is preserved. As an additional confirmation of this interpretation, we have simulated thicker

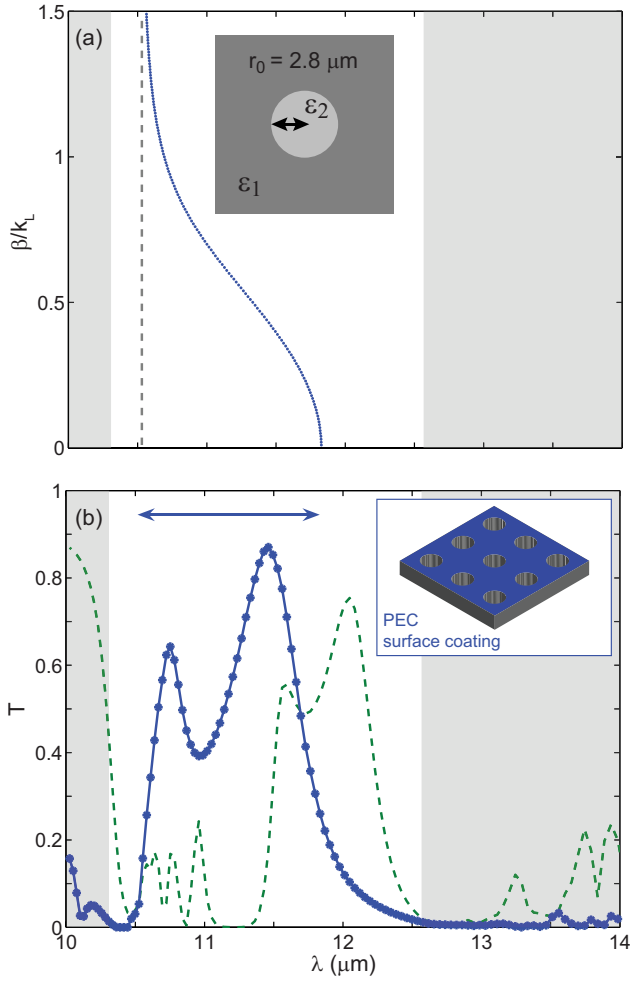

FIG. 4. (Color) (a) Dispersion relation for the lowest-order propagating mode of a cylindrical air hole of radius $r_0=2.8$ μm surrounded by SiC (solid blue curve). The inset shows the geometry. The surface phonon wavelength for a SiC-air interface is indicated by the dashed gray curve. (b) Transmission spectrum for a SiC film ($h=4$ μm) with a 200 nm PEC coating and with a two-dimensional periodic arrangement of subwavelength cylindrical holes (solid blue curve). The inset shows the geometry with the PEC coating indicated in blue. The transmission spectrum in Fig. 1 is shown for reference (dashed green curve).

structures (Fig. 5). We observe that while the spectral range of the high-transmission window remains unchanged, the structure exhibits more Fabry-Pérot oscillations in the spectrum that match well with the dispersion relation of the hole.

(b) Transmission is completely suppressed from 11.08 to 11.33 μm. This feature arises due to Fano interference[21] of the two transmission pathways formed by propagating modes in the holes and surface resonances on the interfaces. The existence of each individual pathway in this spectral region is evident from the results shown in Figs. 3 and 4.

As an intuitive model based on Fano interference analysis, we express the transmitted amplitude t as the sum of two distinct contributions,

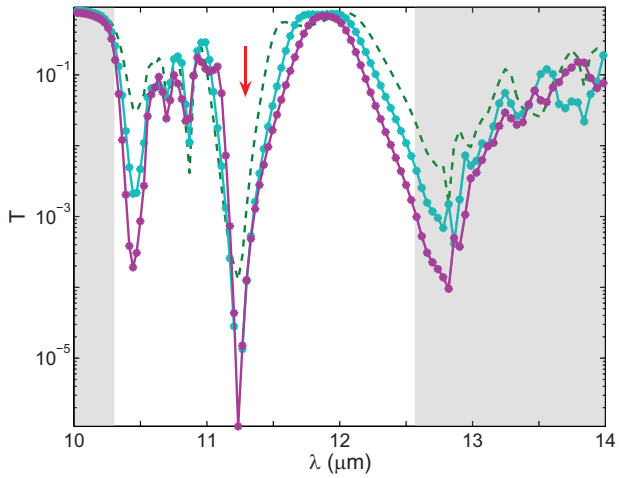

FIG. 5. (Color) Transmission spectrum for SiC films of varying thicknesses ($h=4$ μm, dashed green curve; $h=6$ μm, solid cyan curve; and $h=8$ μm, solid magenta curve) with a two-dimensional periodic arrangement of subwavelength cylindrical holes (radius $r_0=2.8$ μm and period $a=10.4$ μm). The surface resonance is indicated by the red vertical arrow.

$$t = t_d + f\frac{\gamma}{i(\omega-\omega_0)+\gamma}, \tag{4}$$

where t_d is a direct transmission coefficient attributed to the propagating mode and the second term is the contribution of the surface resonance with center frequency ω_0, width γ, and complex amplitude f. Here, we show that this model provides a semiquantitative description of the interplay and gives quantitative results for the enhanced transmission when the propagating modes inside the holes or the surface resonances on the interfaces occur by themselves.

Direct transmission due to the propagating mode provides a broad high-transmission background. If we neglect losses and we assume for simplicity that $t_d \approx 1$, it can be shown that $f \approx -1$ in the region of interest.[22] In this case, the transmission coefficient becomes

$$t \approx \frac{i(\omega-\omega_0)}{i(\omega-\omega_0)+\gamma}, \tag{5}$$

which yields complete suppression $t \approx 0$ at the surface resonance frequency $\omega=\omega_0$. This is precisely what we observe near 11.36 μm (vertical red arrow) in the transmission spectrum of Fig. 2. Our model also implies that the destructive interference leading to complete suppression is largely insensitive to thickness variations of the film. This can be understood by realizing that the direct transmission pathway provides a broad background and remains high for different thicknesses. This behavior is confirmed by FDTD transmission calculations (Fig. 5). In particular, we point to the perfect alignment of the large dip in the transmission spectra near 11.36 μm and the location of the surface resonance (vertical red arrow).

The intuitive model also provides quantitative support for the reported behavior for each of the contribution pathways separately. In the absence of a surface resonance, $f=0$; i.e.,

there is no indirect pathway and the model quantitatively predicts $t=t_d$. This is corroborated by the excellent agreement between the region of enhanced transmission and the range predicted by the dispersion relation of a single hole in Fig. 4. The absence of a propagating mode in the hole, on the other hand, yields a low background $t_d \approx 0$. The analysis results in

$$t \approx \frac{\gamma}{i(\omega - \omega_0) + \gamma}, \tag{6}$$

which yields a near-complete transmission $t \approx 1$ at the surface resonance frequency $\omega = \omega_0$.[22] This agrees with the presence of a transmission peak near 11.36 μm (vertical red arrow) in the transmission spectrum of Fig. 3. Specifically, when δ is a measure of the relative strength of the indirect pathway (surface resonance) to the direct pathway (propagating mode), the complex amplitude of the resonant mode is given by $f=-(1-i\delta/\gamma)t_d$. Here also, Fano interference analysis results in a quantitative model for the surface resonance peak at 11.36 μm (Fig. 3, black dots), which is in excellent agreement with the FDTD calculation (Fig. 3, red solid curve).

As a side note, Fano interference has also been observed in plasmon-polaritonic systems,[23,24] where interfering pathways were identified as evanescently decaying modes and surface resonances.[25,26] However, evanescently decaying modes alone produce a very weak transmission, which is accounted for in the Fano interference model by a very small t_d. Thus, by comparing Eqs. (5) and (6), it can be seen that the details of the Fano interference behavior are, in fact, quite different in the phonon-polaritonic and the plasmon-polaritonic cases, respectively.

Phonon-polaritonic systems, in general, are of great emerging interest,[27–30] since they offer stronger, sharper resonances than metallic systems.[10] The results presented in this work highlight the intricate and unique interplay between surface resonances and propagating modes in phonon-polaritonic systems. We contrast this behavior to that of surface plasmons in metallic systems. Our work also suggests a different application of phonon-polaritonic systems in controlling the near-field of midinfrared light.

This work was supported in part by the Stanford Global Climate and Energy Project (GCEP). The computation is performed through the support of the NSF-LRAC program. The authors acknowledge Hocheol Shin for assistance with computations and Michelle Povinelli and Zheng Wang for discussions.

[1] T. W. Ebbesen, H. J. Lezec, H. F. Ghaemi, T. Thio, and P. A. Wolff, Nature (London) **391**, 667 (1998).
[2] T. Thio, K. M. Pellerin, R. A. Linke, H. J. Lezec, and T. W. Ebbesen, Opt. Lett. **26**, 1972 (2001).
[3] S. Blair and A. Nahata, Opt. Express **12**, 3618 (2004).
[4] E. Popov, M. Neviere, S. Enoch, and R. Reinisch, Phys. Rev. B **62**, 16100 (2000).
[5] L. Martin-Moreno, F. J. Garcia-Vidal, H. J. Lezec, K. M. Pellerin, T. Thio, J. B. Pendry, and T. W. Ebbesen, Phys. Rev. Lett. **86**, 1114 (2001).
[6] M. M. J. Treacy, Phys. Rev. B **66**, 195105 (2002).
[7] H. J. Lezec and T. Thio, Opt. Express **12**, 3629 (2004).
[8] J. Gomez Rivas, M. Kuttge, P. Haring Bolivar, H. Kurz, and J. A. Sanchez-Gil, Phys. Rev. Lett. **93**, 256804 (2004).
[9] J. B. Pendry, L. Martin-Moreno, and F. J. Garcia-Vidal, Science **305**, 847 (2004).
[10] R. Hillenbrand, T. Taubner, and F. Keilmann, Nature (London) **418**, 159 (2002).
[11] S. M. Williams, A. D. Stafford, K. R. Rodriguez, T. M. Rogers, and J. V. Coe, J. Phys. Chem. B **107**, 11871 (2003).
[12] C. Kittel, *Introduction to Solid State Physics* (Wiley, New York, 1996).
[13] W. G. Spitzer, D. Kleinman, and D. Walsh, Phys. Rev. **113**, 127 (1959).
[14] A. Taflove and S. C. Hagness, *Computational Electrodynamics: The Finite-Difference Time-Domain Method* (Artech House, Boston, 2000).
[15] K. J. Klein Koerkamp, S. Enoch, F. B. Segerink, N. F. van Hulst, and L. Kuipers, Phys. Rev. Lett. **92**, 183901 (2004).
[16] H. Shin, P. B. Catrysse, and S. Fan, Phys. Rev. B **72**, 085436 (2005).
[17] Rayleigh, Proc. R. Soc. London, Ser. A **79**, 399 (1907).
[18] R. W. Wood, Philos. Mag. **3**, 396 (1902).
[19] S. Enoch, E. Popov, M. Neviere, and R. Reinisch, J. Opt. A, Pure Appl. Opt. **4**, S83 (2002).
[20] D. M. Pozar, *Microwave Engineering* (Wiley, New York, 1998).
[21] U. Fano, Phys. Rev. **124**, 1866 (1961).
[22] S. H. Fan and J. D. Joannopoulos, Phys. Rev. B **65**, 235112 (2002).
[23] C. Ropers, D. J. Park, G. Stibenz, G. Steinneyer, J. Kim, D. S. Kim, and C. Lienau, Phys. Rev. Lett. **94**, 113901 (2005).
[24] F. Marquier, J. J. Greffet, S. Collin, F. Pardo, and J. L. Pelouard, Opt. Express **13**, 70 (2005).
[25] C. Genet, M. P. van Exter, and J. P. Woerdman, Opt. Commun. **225**, 331 (2003).
[26] M. Sarrazin, J. P. Vigneron, and J. M. Vigoureux, Phys. Rev. B **67**, 085415 (2003).
[27] J. J. Greffet, R. Carminati, K. Joulain, J. P. Mulet, S. P. Mainguy, and Y. Chen, Nature (London) **416**, 61 (2002).
[28] K. C. Huang, P. Bienstman, J. D. Joannopoulos, K. A. Nelson, and S. Fan, Phys. Rev. Lett. **90**, 196402 (2003).
[29] G. Shvets, Phys. Rev. B **67**, 035109 (2003).
[30] F. Marquier, K. Joulain, and J. J. Greffet, Opt. Lett. **29**, 2178 (2004).